

Spectral analysis of wetlands using multi-source optical satellite imagery

Meisam Amani^{a,b,*}, Bahram Salehi^{a,b}, Sahel Mahdavi^{a,b}, Brian Brisco^c

^a C-CORE, Morrissey Road, St John's, NL A1B 3X5, Canada

^b Department of Electrical and Computer Engineering, Faculty of Engineering and Applied Science, Memorial University of Newfoundland, St John's, NL A1C 5S7, Canada

^c The Canada Center for Mapping and Earth Observation, Ottawa, Ontario K1S 5K2, Canada



ARTICLE INFO

Keywords:

Remote sensing
Wetlands
Spectral analysis
Separability measures
Canada

ABSTRACT

The separability of wetland types using different spectral bands is an important subject, which has not yet been well studied in most countries. This is particularly of interest in Canada because it contains approximately one-fourth of the total global wetlands. In this study, the spectral separability of five wetland classes, namely Bog, Fen, Marsh, Swamp, and Shallow Water, was investigated in Newfoundland and Labrador (NL), Canada, using field data and multi-source optical Remote Sensing (RS) images. The objective was to select the most useful spectral bands for wetland studies from four commonly used optical satellites: RapidEye, Sentinel 2A, ASTER, and Landsat 8. However, because the ultimate objective was the classification of wetlands in the province, the separability of wetland classes was also evaluated using several other features, including various spectral indices, as well as textural and ratio features to obtain a high level of classification accuracy. For this purpose, two separability measures were used: The T-statistics, calculated from the parametric *t*-test method, and the U-statistics, derived from the non-parametric Mann-Whitney U-test. The results indicated that the Near Infrared (NIR) band was the best followed by the Red Edge (RE) band for the discrimination of wetland class pairs. The red band was also the third most useful band for separation of wetland classes, especially for the delineation of the Bog class from the other types. Although the Shortwave Infrared (SWIR) and green bands demonstrated poor separability, they were comparatively more informative than the Thermal Infrared (TIR) and blue bands. This study also demonstrated that ratio features and some spectral indices had high potential to differentiate the wetland species. Finally, wetlands in five study areas in NL were classified by inserting the best spectral bands and features into an object-based Random Forest (RF) classifier. By doing so, the mean Overall Accuracy (OA) and Kappa coefficient in the study areas were 86% and 0.82, respectively.

1. Introduction

Wetlands are valuable natural resources that provide many ecological services to both flora and fauna. Their benefits are a result of the natural hydrological and biogeochemical processes carried out in these ecosystems. These processes, which are sometimes called wetland functions, include hydraulic storage and recharge, bio-geochemical transformation, biomass production, and habitat (Marton et al., 2015). In addition, these habitats are important forms of economic resources in many countries in the form of recreation, fishing, waterfowl hunting, and animal grazing (Marton et al., 2015; Guo et al., 2017). In recent times, wetlands have also become a popular topic in discussions of climate change because they contain 12% of the global carbon pool (Erwin, 2009; Guo et al., 2017).

Because of the valuable services that wetlands provide, the Ramsar Convention carried out a review of wetland inventories across the globe

in an effort to analyze the extent, status, and effectiveness of inventories around the world, and to provide several specific recommendations as to how different countries can establish or improve on these important wetland tools (Finlayson et al., 1999). Consequently, attempts have been made to develop a wetland classification system based on the specific types of wetlands in each country (Ozesmi and Bauer, 2002; Tiner et al., 2015; Guo et al., 2017; Mahdavi et al., 2017b). For instance, there are two well-known wetland classification systems in Canada (National Wetlands Working Group, 1987; Smith et al., 2007): the Canadian Wetland Classification System (CWCS, refer to Table 1 for the list of acronyms) and the Enhanced Wetland Classification System (EWCS). The CWCS is the only Canada-wide classification system, which incorporates ecological characteristics of wetlands and their functions into the classification (National Wetlands Working Group, 1987). The CWCS categorizes wetlands into five classes based on their soil, water, and vegetation characteristics: Bog, Fen, Marsh, Swamp,

* Corresponding author at: C-CORE, Memorial University of Newfoundland, Morrissey Road, St John's, NL A1B 3X5, Canada.

E-mail address: ma3780@mun.ca (M. Amani).

Table 1

Acronyms and corresponding description.

Acronyms	Description
ASTER	Advanced Spaceborne Thermal Emission and Reflection Radiometer
B	Band
CWCS	Canadian Wetland Classification System
DEM	Digital Elevation Model
DVI	Difference Vegetation Index
EWCS	Enhanced Wetland Classification System
F-test	Fisher-test
ML	Maximum Likelihood
NIR	Near Infrared
NL	Newfoundland and Labrador
NDSI	Normalized Difference Soil Index
NDVI	Normalized Difference Vegetation Index
NDWI	Normalized Difference Water Index
OBIA	Object-Based Image Analysis
OA	Overall Accuracy
PA	Producer Accuracy
RF	Random Forest
RE	Red Edge
RE-NDVI	Red Edge Normalized Difference Vegetation Index
RS	Remote Sensing
SWIR	Shortwave Infrared
SAVI	Soil Adjusted Vegetation index
SAM	Spectral Angle Mapper
SAR	Synthetic Aperture RADAR
TIR	Thermal Infrared
UA	User Accuracy

and Shallow water. Table 2 summarizes the ecological characteristics of these five wetland classes (National Wetlands Working Group, 1987; Mitsch and Gosselink, 2000; Smith et al., 2007), which provides the framework for analyzing the spectral characteristics of wetlands.

The characteristics and properties of wetlands can be effectively studied by measuring the spectral response of wetland types in different parts of the electromagnetic spectrum (Ozesmi and Bauer, 2002; Mahdavi et al., 2017b). In this regard, collecting the spectral information of wetlands can be performed using field spectrometry. However, besides the common limitations of field work (e.g. labor intensiveness, high expenses, and time limitation), inaccessibility has proven to be a major disadvantage when collecting wetland ground-truth data (Adam and Mutanga, 2009; Gallant, 2015; Mahdavi et al., 2017b). Because of these limitations, there is a need to develop a more effective and practical approach for analyzing the spectral characteristics of wetlands. In this regard, using the data collected by various optical RS satellites, characterized by different spatial, temporal, and spectral resolutions, is an optimum way to study the spectral characteristics of wetlands (Ozesmi and Bauer, 2002; Gallant, 2015; Tiner et al., 2015; Guo et al., 2017; Mahdavi et al., 2017b).

Optical RS supplies images in various parts of the electromagnetic spectrum, including the visible and infrared (near, shortwave, and thermal). It should be noted that RS-based spectral analysis of wetlands requires knowledge of the spectral characteristics of vegetation and soils, as well as their correspondence with the vegetation cover and soil conditions in wetland areas (see National Wetlands Working Group (1987) for the characteristics of wetland species). Hyperspectral sensors may be the best choice for spectral analysis of wetlands. However, the corresponding data are generally expensive and difficult to obtain and process (Guo et al., 2017). Moreover, since there are not current hyperspectral orbital assets, it is necessary to figure out how to perform this using multispectral data. In addition, most current wetland inventories are based on the data acquired by multi-spectral satellites such as Landsat (Ozesmi and Bauer, 2002; Guo et al., 2017; Mahdavi et al., 2017b). Moreover, there are currently many satellites, which provide valuable multi-spectral imagery for users free of charge, including Landsat, Sentinel 2A, and Advanced Spaceborne Thermal Emission and Reflection Radiometer (ASTER). Thus, it is often more

Table 2
The characteristics of the five wetland classes specified by the CWCS.

Wetland class	Characteristics		Hydrology	Soil	pH	Nutrient conditions	Vegetation physiognomy
	Water source	Water table					
Bog	Ombrogenous	At or slightly below the surface	May have standing water	Organic	Acidic	Oligotrophic	Byrophytes (sphagnum moss), graminoids (sedges), ericaceous shrubs
Fen	Minerogenous	Fluctuating (at, slightly above, or slightly below the ground surface)	Standing or gently flowing water	Organic	Acidic to alkaline	Eutrophic, mesotrophic, oligotrophic	Bryophytes (brown and sphagnum mosses), graminoids (sedges), shrubs
Marsh	Minerogenous	At or below the ground surface	Standing or flowing water with fluctuating water levels	Mineral	Neutral to alkaline	Usually eutrophic	Aquatic emergent graminoids and shrubs
Swamp	Minerogenous	At or below the ground surface	Seasonal standing or flowing water	Organic or mineral	Alkaline to slightly acidic	Eutrophic, mesotrophic, oligotrophic	Trees and shrubs greater than 1 m, forbs
Shallow Water	Minerogenous	At the surface	Seasonally stable standing or flowing water < 2 m	Mineral	Neutral to alkaline	Usually eutrophic	Submerged and floating aquatic macrophytes

Note: Water Source: The source of water that feeds a wetland. Ombrogenous wetlands receive water only from precipitation (rain, snow, and atmosphere), while Minerogenous wetlands receive water from multiple sources (e.g. precipitation and surface water flow).

Water Table: The upper portion of the zone of saturation, which is the area underground where the ground is totally saturated by water.

Soil: Wetland soils can be broadly defined as being Organic or Mineral. Organic soil is a result of a buildup of poorly decomposed organic (carbon) matter, while Mineral soil contains little or no organic matter, and can be described as mucky.

Nutrient conditions: General nutrient quality of the wetland. Oligotrophic wetlands are poor in nutrients, mesotrophic wetlands have moderate levels of nutrients, and eutrophic wetlands have high levels of nutrients. Vegetation physiognomy: Describes the functional and morphological attributes of vegetation (e.g. shrubs have woody stems, and macrophytes are aquatic plants).

practical to use multi-spectral satellite data for wetland mapping, instead of hyperspectral data (Ozesmi and Bauer, 2002; Guo et al., 2017; Mahdavi et al., 2017b).

When using multi-spectral data, it is important to investigate the different spectral bands of satellites to see which provide the best separability for the wetland classes. Several studies have been conducted in this regard, most of which have argued that the Near Infrared (NIR) and Red Edge (RE) bands are the most useful for delineation of wetland types (Schmidt and Skidmore, 2003; Ozesmi and Bauer, 2002; Adam et al., 2010; Mutanga et al., 2012; Amani et al., 2017a; Mahdavi et al., 2017b). The Shortwave Infrared (SWIR) bands, which are sensitive to both soil and vegetation moisture, have also been reported to be useful for discriminating some wetland types (Crist and Cicone, 1984; Mahdavi et al., 2017b). Moreover, Thermal Infrared (TIR) bands have distinguished water bodies from vegetation and soil covers (Amani et al., 2017a; Mahdavi et al., 2017b). The TIR bands has also been reported to be helpful in identifying inundated wetlands (Leblanc et al., 2011; Mahdavi et al., 2017b).

There are currently many optical satellites that provide medium to high spatial resolution images. These data can be effectively used to obtain detailed information from wetlands. Furthermore, through the availability of medium and high spatial resolution imagery, the Object-Based Image Analysis (OBIA) can be applied in place of traditional pixel-based methods for wetlands classification. The OBIA works by grouping homogenous pixels to produce image objects and, then, uses the spatial, spectral, as well as topological features of objects to improve classification accuracy (Hay and Castilla, 2008). Many researchers have reported that the OBIA is superior to the pixel-based methods in wetland classification (e.g., Harken and Sugumaran, 2005; Laba et al., 2010; Mahdianpari et al., 2018; Mahdavi et al., 2017a; Amani et al., 2017b,c). For instance, Harken and Sugumaran (2005) compared the pixel-based Spectral Angle Mapper (SAM) method and a non-parametric object-based classification for wetlands classification in Iowa, USA. They applied hyperspectral imagery to overcome the limitation of multi-spectral data in providing the spectral information of wetlands, and obtained 92% and 64% Overall Accuracy (OA) using the OBIA and SAM, respectively. Laba et al. (2010) also used the IKONOS imagery for wetlands classification in Tivoli Bays, New York, and demonstrated that wetland classification accuracy can be improved by including object-based textural features to a pixel-based Maximum Likelihood (ML) classifier. Moreover, Amani et al. (2017b) compared the results of OBIA with pixel-based classification in Newfoundland and Labrador (NL), Canada, and concluded that all wetland classes were identified more correctly using the OBIA method in terms of both visual appearance and statistical accuracies.

Considering important values of wetlands in Canada, currently, there are no comprehensive studies from Canada that analyze the spectral characteristics of wetlands using optical satellites. This study aims to investigate the separability of five wetland classes as defined by the CWCS using a combination of field data and multi-source optical satellite images. Other spectral features, including the textural and ratio features, as well as various spectral indices were also evaluated to select the most important features for discriminating different wetland class pairs. Finally, a combination of the best spectral bands and features was inserted to an object-based Random Forest (RF) algorithm to classify wetlands in five different study areas with various ecologies across NL, Canada.

2. Study area and data

2.1. Study areas

This research was carried out in five study areas (each approximately 700 km²) distributed across NL, Canada (Fig. 1). The locations of these study areas were based on the following considerations:

- (1) For timely and efficient field work and to increase the visitation of as many wetlands as possible, the areas were located in proximity to populated areas where road access to a large amount of the study area is available.
- (2) Because NL has a largely variable geology and climate considering its size of 106,000 km² (South, 1983), the five study areas were selected to represent the islands regional variation in landscape and vegetation as adequate as possible.
- (3) Ancillary data, such as aerial photos, archived land cover maps, and Digital Elevation Model (DEM) were available from the study areas.

The Avalon study area is located on the north-east portion of the Avalon Peninsula, on the south-east of Newfoundland, and is situated around the capital city of St. John's. Since the area is located in the Maritime Barrens ecoregion, it experiences an oceanic climate of foggy cool summers and short winters (Ecological Stratification Working Group, 1996). The landscape is also characterized by balsam fir forests, heathland dominated by ericaceous shrubs, moss, bogs, fens, and lichen (South, 1983; Ecological Stratification Working Group, 1996), and the largest urban area presence in the province.

Closest to the Avalon is the Grand Falls-Windsor study area, in north-central Newfoundland. Being situated in the Central Newfoundland ecoregion, this study area experiences a continental climate specified by cool summers and cold winters (Ecological Stratification Working Group, 1996). In addition, the landscape is dominated by forests of balsam fir and black spruce, kalmia heathland, peatland (South, 1983; Ecological Stratification Working Group, 1996), and several urban areas.

The Deer Lake study area is approximately 130 km west of Grand-Falls Windsor, within the same Central Newfoundland ecoregion characterized by a continental climate (Ecological Stratification Working Group, 1996). Major land cover includes balsam and black spruce forest and peatlands (South, 1983). There is comparatively minor portions of urban areas within this study area, with only the small settlement of Howley within its borders.

The Gros Morne study area is located on the west coast of Newfoundland on the Great Northern Peninsula, adjacent to the Gulf of St. Lawrence. The study area falls in the Northern Peninsula ecoregion, which has an oceanic climate and experiences wind and fog (Ecological Stratification Working Group, 1996). In this study area, land cover is dominated by extensive low-lying peatlands (South, 1983). Moreover, moving east across the study area, the elevation dramatically increases, and the mountainous areas are covered in balsam fir and black spruce forests (South, 1983). Additionally, the Gros Morne National Park is located within the study area boundaries, as are several small communities, including Cow Head.

Goose Bay is the only study area located on the mainland near Happy Valley-Goose Bay, the largest town in Labrador. This study area falls within the Lake Melville ecoregion, characterized by humid but cool summers and cold winters (South, 1983). The landscape is covered by balsam fir, black spruce, white birch trees, and large portions of lichen dominated woodland. Furthermore, permafrost within wetlands is common in this study area due to the northern temperatures (Ecological Stratification Working Group, 1996).

2.2. Field data

The field work was conducted in all five study areas between July and October of 2015 and June and August of 2016 by 4 field teams made up of biologists and wetland ecologists. The goal of the field work was to ground-truth and classify five wetland types to act as testing and training data for the development of methods for the remote classification of wetlands across NL. Potential wetland sites within each study area were selected for investigation using the visual analysis of aerial and satellite imagery in the study areas. The requirements for site selection were as follows:

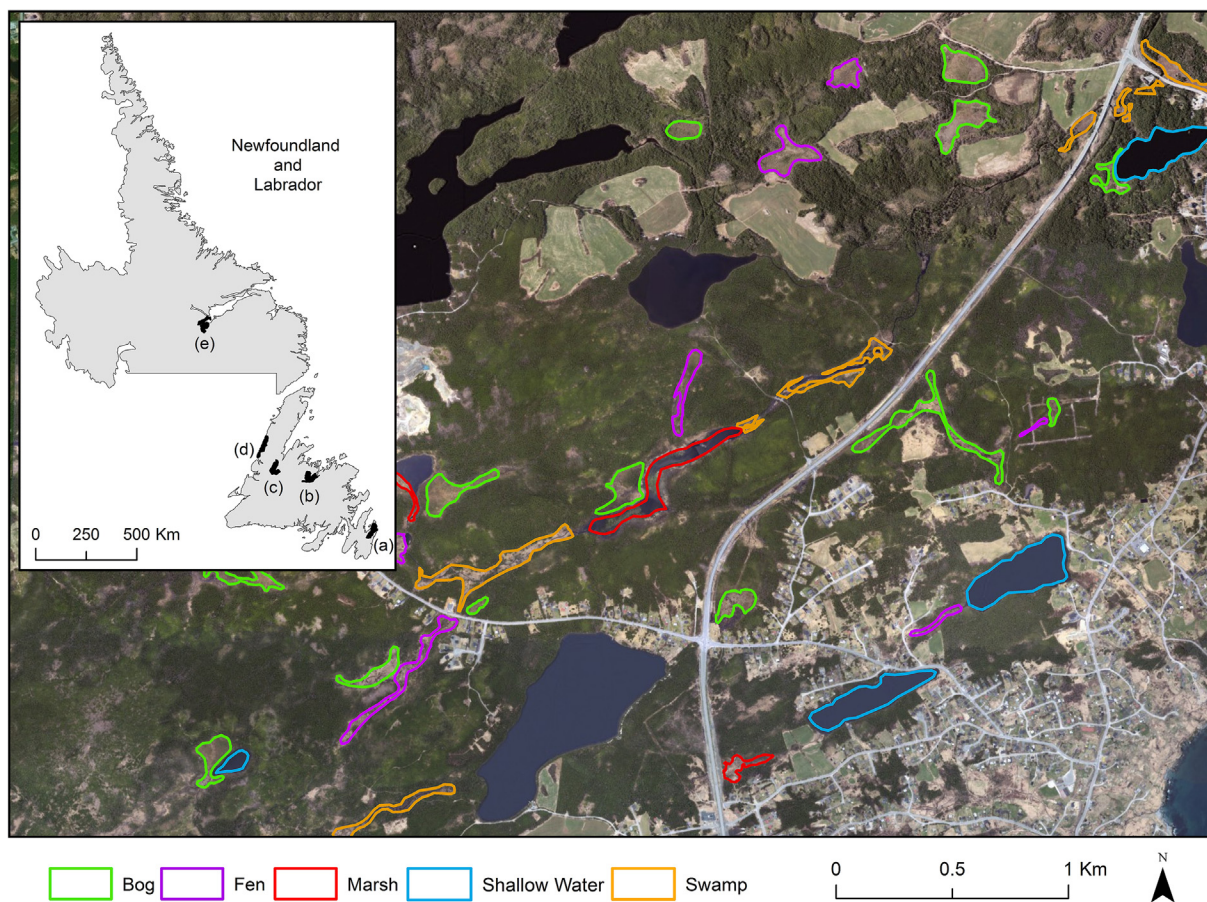


Fig. 1. The upper left image illustrates the province of Newfoundland and Labrador, as well as the five study areas: (a) Avalon, (b) Grand Falls-Windsor, (c) Deer Lake, (d) Gros Morne, and (e) Goose Bay. The zoomed image also demonstrates the boundaries of different wetland classes obtained from the field work conducted in the Avalon study area.

- (1) The site must be within 200 m of public road and pathways for ease-of accessibility.
- (2) The site should be located on public land.
- (3) The site must be a good example of one of the five wetland classes described by the CWCS.

If the visited site was in-fact a wetland, it was: (1) classified following the CWCS key, (2) one or several GPS points were collected within or as close to the wetland as possible, (3) several pictures were taken, and (4) ancillary notes, including information on the dominant vegetation, hydrology, and surrounding upland, were recorded. It is also worth mentioning that there was no restriction on the size of wetlands during the first year (2015) of field work, resulting in several of the classified wetlands being quite small. However, more effort was paid to collecting wetlands of a size > 1 ha where possible during the following year (i.e. 2016).

After completion of the field work, the GPS points were imported into ArcMap 10.3.1. Then, boundary delineation was conducted with the aid of several types of remotely sensed imagery, including high resolution *ortho*-photography, RapidEye imagery, and the satellite imagery base-map provided by Esri through the ArcMap. Boundaries were primarily delineated following the visible transition of dominant vegetation from wetland (the type of vegetation depends on the wetland class) to surrounding upland. Additionally, boundaries were determined conservatively to avoid including transitional areas where wetland vegetation may be mixed with upland vegetation. Table 3 provides the information of the total field samples (polygons) used in this study. It should be noted that the extracted polygons were the base of all analyses conducted in this study.

Table 3
The number of field samples (polygons) collected over five study areas.

Study area	Class	Number of polygons	Area (ha)
Avalon	Bog	83	269
	Fen	39	80
	Marsh	50	62
	Swamp	45	47
	Shallow water	40	110
Grand Falls-Windsor	Bog	30	357
	Fen	61	194
	Marsh	45	102
	Swamp	30	47
	Shallow water	21	52
Deer Lake	Bog	31	236
	Fen	54	121
	Marsh	24	19
	Swamp	40	56
	Shallow water	23	68
Gros Morne	Bog	38	779
	Fen	31	98
	Marsh	31	50
	Swamp	42	48
	Shallow water	27	64
Goose Bay	Bog	28	395
	Fen	29	139
	Marsh	21	78
	Swamp	23	35
	Shallow water	11	19

Table 4

The satellite data used in this study.

Study area	RapidEye	Sentinel 2A	ASTER	Landsat 8
Avalon	2015/06/18	–	2015/06/05	2015/06/19
Grand Falls-Windsor	2015/06/10	–	–	2015/06/10
Deer Lake	2015/06/18	2016/06/12	–	–
Gros Morne	2015/06/18	2016/06/25	2015/06/25	2015/06/15
Goose Bay	–	–	2015/06/23	2015/06/22

2.3. Satellite data

In this study, data collected by four optical satellites, RapidEye, Sentinel 2A, ASTER, and Landsat 8, were investigated in late spring (**Table 4**). June was selected as this was the month that had the greatest amount of satellite data covering each of the study areas available for this research. In addition, each of the selected satellites contains valuable characteristics, which makes them suitable for operational wetland mapping and monitoring (Gallant 2015; Chatziantoniou et al., 2017; Amani et al., 2017b; Araya-López et al., 2018). For example, Gallant (2015) has mentioned that Landsat sensors have been traditionally popular for wetland mapping because of their rich temporal archive, wide coverage, and no cost for users. Moreover, except for RapidEye, the images captured by the other three satellites are freely available for users and, therefore, are appropriate for regional and national wetland studies. It is worth noting that since the images were acquired at different times (between June 5 and 25), various solar zenith angles can affect the results slightly, which was not considered in this study.

The characteristics of the applied spectral bands are also demonstrated in **Table 5**. According to this table, different spectral bands covering various parts of the electromagnetic spectrum, including visible, NIR, SWIR, as well as TIR, were evaluated for separability analysis of wetlands in this study. It should be noted that because of the uncertainties involved with the SWIR bands of ASTER (bands 4–9) and the TIR band (band 11) of Landsat 8, they were excluded from this study. Moreover, the aerosol, water vapor, and cirrus bands of Sentinel 2A (bands 1, 9, and 10) and Landsat 8 (bands 1 and 9) are inappropriate for separability analysis of wetlands and, thus, were not investigated.

3. Methods

3.1. Preprocessing of satellite data

Since all the images were already geometrically corrected with accuracy of less than one pixel size, no further geometric corrections were carried out. Regarding the radiometric and atmospheric correction of the satellite data, the following steps were performed on each optical imagery to obtain the surface reflectance and temperature values.

(1) The RapidEye surface reflectance data were derived using the

Table 5

The spectral bands of RapidEye, Sentinel 2A, ASTER, and Landsat 8 used in this study (The wavelength range for each band is provided in the parentheses, and is in micrometers).

RapidEye	Sentinel 2A	ASTER	Landsat 8
B1_Blue (0.44–0.51)	B2_Blue (0.46–0.52)	B1_Green (0.52–0.6)	B2_Blue (0.45–0.51)
B2_Green (0.52–0.6)	B3_Green (0.54–0.58)	B2_Red (0.63–0.69)	B3_Green (0.53–0.59)
B3_Red (0.63–0.69)	B4_Red (0.65–0.68)	B3N_NIR (0.76–0.86)	B4_Red (0.64–0.67)
B4_RE (0.69–0.73)	B5_RE (0.698–0.712)	B10_TIR (8.13–8.48)	B5_NIR (0.85–0.88)
B5_NIR (0.76–0.85)	B6_RE (0.733–0.747)	B11_TIR (8.48–8.83)	B6_SWIR (1.57–1.67)
	B7_RE (0.773–0.793)	B12_TIR (8.93–9.28)	B7_SWIR (2.11–2.29)
	B8_NIR (0.784–0.9)	B13_TIR (10.25–10.95)	B10_TIR (10.6–11.19)
	B8A_RE (0.855–0.875)	B14_TIR (10.95–11.65)	
	B11_SWIR (1.565–1.655)		
	B12_SWIR (2.1–2.28)		

Table 6

The spectral indices, textural and ratio features evaluated in this study for separability analyses of wetland types.

Spectral indices	$\text{Brightness, NDWI} = \frac{\text{Green} - \text{NIR}}{\text{Green} + \text{NIR}}$, $\text{DVI} = \text{NIR} - \text{Red}$, $\text{NDVI} = \frac{\text{NIR} - \text{Red}}{\text{NIR} + \text{Red}}$, $\text{RE-NDVI} = \frac{\text{NIR} - \text{RE}}{\text{NIR} + \text{RE}}$, $\text{NDSI} = \frac{\text{SWIR} - \text{NIR}}{\text{SWIR} + \text{NIR}}$, $\text{SAVI} = \frac{(1 + L)(\text{NIR} - \text{Red})}{\text{NIR} + \text{Red} + L}$
Ratio features	$\frac{\text{Blue}}{\text{Brightness}}$, $\frac{\text{Green}}{\text{Brightness}}$, $\frac{\text{Red}}{\text{Brightness}}$, $\frac{\text{RE}}{\text{Brightness}}$, $\frac{\text{NIR}}{\text{Brightness}}$, $\frac{\text{SWIR}}{\text{Brightness}}$
Texture features	Standard deviation of the polygons obtained from all spectral bands of the satellites.

Atmospheric and Topographic Correction Software (ATCORE) module of the PCI Geomatica software. The procedure is explained in details in Richter (2011).

- (2) The top of atmosphere reflectance Sentinel 2A data (Level 1C products) were first downloaded from <https://scihub.copernicus.eu/>. Then, these datasets were converted to surface reflectance data using the Sen2Cor version 2.3.1 radiative transfer atmospheric correction code (downloaded from the website of ESA Science Toolbox Exploitation Platform (STEP): <http://step.esa.int/main/third-party-plugins-2/sen2cor/>). More details regarding the Sen2Cor processing can be found in Gascon et al. (2017) and Li et al. (2018).
- (3) The ASTER level 2 surface reflectance products (AST_07XT) were used in this study (https://lpdaac.usgs.gov/dataset_discovery/aster/aster_products_table/ast_07xt_v003; Iwasaki and Tonooka, 2005). Regarding the thermal bands of ASTER, the level 2 Land Surface Temperature (LST) products (AST_08) were used (https://lpdaac.usgs.gov/dataset_discovery/aster/aster_products_table/ast_08_v003).
- (4) The Landsat 8 surface reflectance data (level 2 products) were downloaded from <https://espa.cr.usgs.gov>, and were used. The Single-Channel method was also implemented to derive the LST values from the band 10 of Landsat 8.

3.2. Variance analyses of field samples

Field samples collected for RS applications should contain the highest possible accuracy. However, since wetlands are complex environments and each wetland class can contain several subclasses (National Wetlands Working Group, 1987), the spectral responses of different field samples within one wetland type can vary considerably. Consequently, when analyzing the spectral responses of different field samples from a particular wetland class, the values may not be in the same range and a large variance can be observed. Therefore, the variation of different field samples from each wetland class should be initially analyzed. To do this, the variance value of samples in each spectral band was calculated for each wetland class using Eq. (1). Then, the spectral bands for which the field samples' values had significant

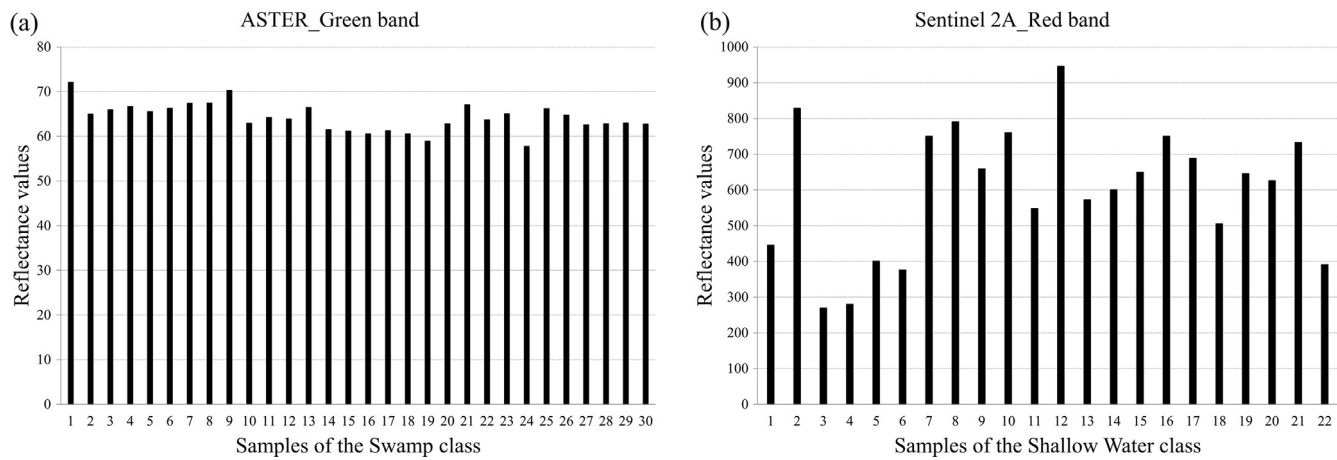


Fig. 2. Spectral values of the field samples of two wetland classes.

variation were removed from the rest of the analyses.

$$Var = \frac{1}{N-1} \sum_{i=1}^N (x_i - \mu)^2 \quad (1)$$

in which x_i indicates the value of a field sample, μ is the mean value of samples, and N is the number of field samples in a spectral band.

After analyzing the variance values of the field samples in individual classes, the variations of field samples within a spectral band were investigated for wetland class pairs. In fact, before performing any separability analysis of different classes in an image using spectral bands, we should be certain whether the classes of interest are separable using the applied spectral bands. This matter is more important for some RS applications, such as wetland classification, where the spectral characteristics of various field samples are different for a wetland class, as explained above. To be more precise, when analyzing the separability of two wetland classes using any spectral band, the variance value of field samples must be greater between rather than within classes in that particular band. To explore this, the Fisher-test (*F*-test) statistics (Eq. (2)) was used and evaluated for each pair of wetland classes. Then, if the *F*-test value was less than one, we removed that spectral band for the class pairs from the subsequent analyses.

$$F = \frac{Var_B}{Var_W} \quad (2)$$

where Var_B and Var_W indicate the between and within variance values in each class pair, respectively. It is also worth mentioning that the *F*-test statistics can also be used for separability analysis, in which the class pair that has higher values in spectral band(s) will be more separable using the corresponding band(s).

3.3. Separability measures

So far, different separability measures have been developed and applied to perform feature selection with inconsistent results in RS science. It has been frequently acknowledged that there is not a unique separability measure to select the most useful spectral band(s) for distinguishing various land cover classes (Yeung et al., 2005; Adam et al., 2010; Manevski et al., 2011; Proctor et al., 2013). Therefore, it was difficult to use the best method for selecting the most useful band or band combinations for discriminating different pairs of wetland classes in this study. After studying various separability measures, we ultimately implemented and used two distance measures of the T-statistics and U-statistics, calculated from the parametric *t*-test method and the non-parametric Mann-Whitney U-test method, respectively.

3.3.1. *T*-test

The *t*-test is a parametric test that determines whether the means of

two classes are statistically different (Fay and Proschan, 2010; Mwangi et al., 2014). According to the pair-wised separability analysis in this study, an independent two-sample *t*-test was used. It has been reported that the two-sample *t*-test performs well, provided that the sample size of each class is greater than 15, and regardless of the distribution of data (Minitab, 1991; Ryan and Joiner, 2001). Additionally, the *t*-test is fast and straightforward to implement, and usually has more statistical power than most non-parametric tests (Minitab, 1991; Ryan and Joiner, 2001). The distance measure derived from the *t*-test method (called T-statistics) has different forms based on the assumptions of equal or unequal sample sizes and/or variances (Fay and Proschan, 2010; Mwangi et al., 2014). Since the sample size of various wetland classes in this study differed and the variance values varied significantly (see the previous subsection), the following form of the *t*-statistics, which assumes unequal sample sizes and unequal variances, was employed.

$$T\text{-Statistics} = \frac{|\mu_1 - \mu_2|}{\sqrt{\frac{Var_1}{n_1} + \frac{Var_2}{n_2}}} \quad (3)$$

in which μ_i , Var_i , and n_i indicate the mean, variance, and the number of field samples of class i , respectively.

3.3.2. Mann-Whitney U-test

The Mann-Whitney U-test is a non-parametric method that does not assume a normal distribution for the samples and evaluates the variance values of the data replaced by their ranks. In this method, instead of the difference in mean values, that of the median values of each spectral band is considered (Lehmann, 2004). It has been reported that if the data is assumed to have a normal distribution, the Mann-Whitney U-test has an efficiency of approximately 0.95 compared to the *t*-test (Lehmann, 2004). However, when the distribution is not normal and the sample size is large, the Mann-Whitney U-test is more efficient than the *t*-test (Conover, 1980). Furthermore, unlike parametric methods, the Mann-Whitney U-test is not seriously affected by outliers (Minitab, 1991; Ryan and Joiner, 2001). In this study, the U-statistics calculated from the Mann-Whitney U-test method (Eq. (4)), was used to evaluate the amount of separability between the wetland class pairs.

$$U\text{-Statistics} = \min(U_1, U_2) \quad (4)$$

where U_i is the U value calculated for class i using the following equations:

$$U_1 = n_1 n_2 + \frac{n_1(n_1 + 1)}{2} - R_1 \quad (5)$$

$$U_2 = n_1 n_2 + \frac{n_2(n_2 + 1)}{2} - R_2 \quad (6)$$

in which n_i and R_i are the number of samples and the sum of the ranks

for class i , respectively. It is also worth mentioning that since the number of field samples in this study was more than 20 for all wetland classes, analogous to the non-equal number of samples from each wetland classes did not affect the spectral analyses.

3.4. Separability analyses of other features

The final purpose of this research was the object-based classification of wetlands using multi-source satellite imagery. Although we could insert the most informative spectral bands, obtained from the separability analyses of spectral bands (calculated from the mean values of

field samples), into the classification and produce the classified maps of wetlands, this will not result in the highest classification accuracy. The reason is that there may still be some classes that are not separable using only the mean values of samples. Since the object-based method was used in this study, many features could be considered for separability analysis of different wetlands and, consequently, for wetland classification. Therefore, besides the mean values of spectral bands, various spectral indices, texture and ratio features (Table 6) were also evaluated for distinguishing wetland class pairs, as well as all wetland classes. To do this, the procedures, described in Sections 3.1 and 3.2 were performed on these features.

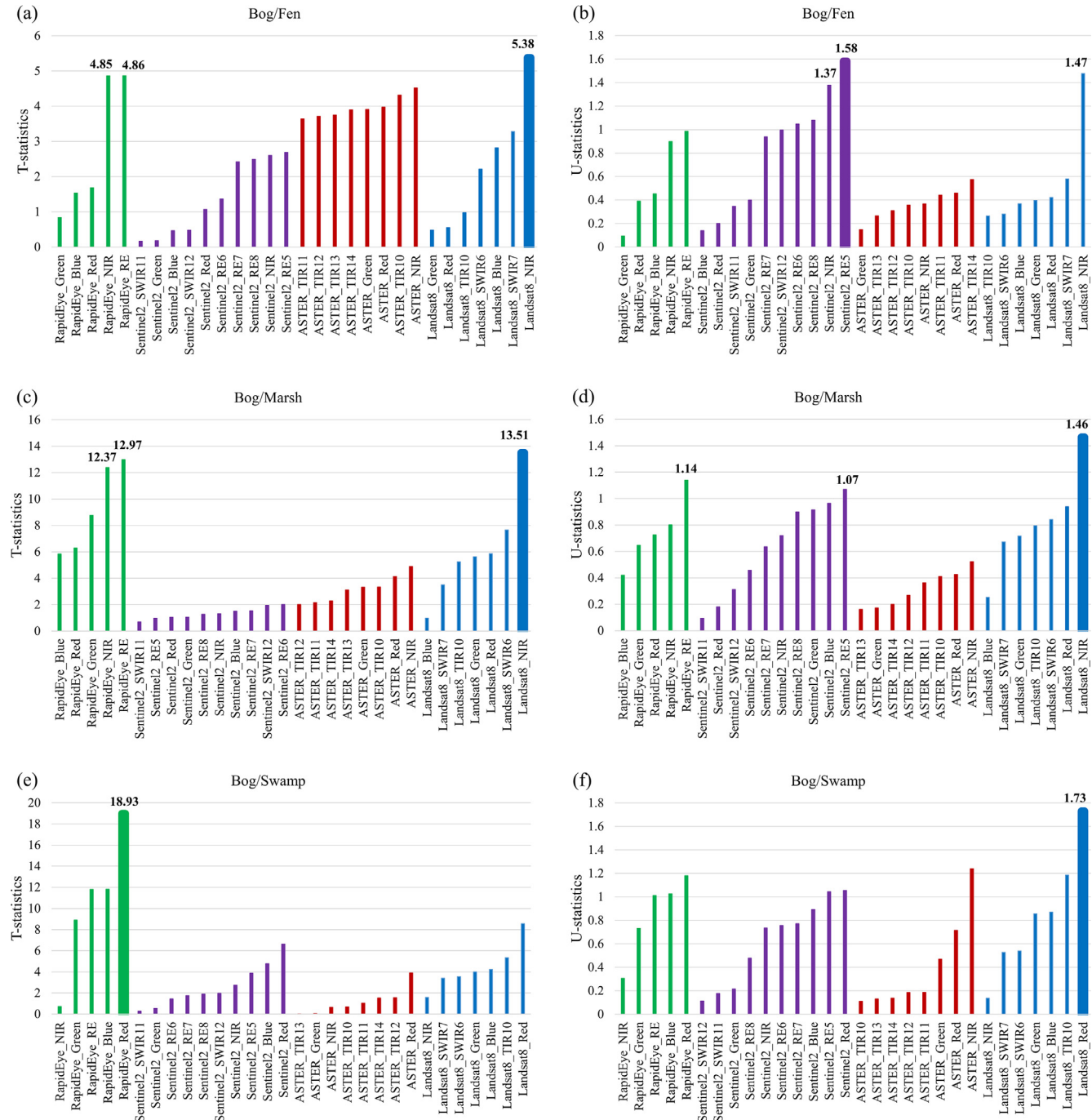


Fig. 3. Separability measures of wetland class pairs in late spring (June) using the T-statistics and U-statistics. In each figure, the spectral band that provides the highest separability is highlighted (The numbers after the name of the spectral bands also indicate the number of the band. For example: ASTER_TIR14 is the TIR band (band 14) of ASTER).

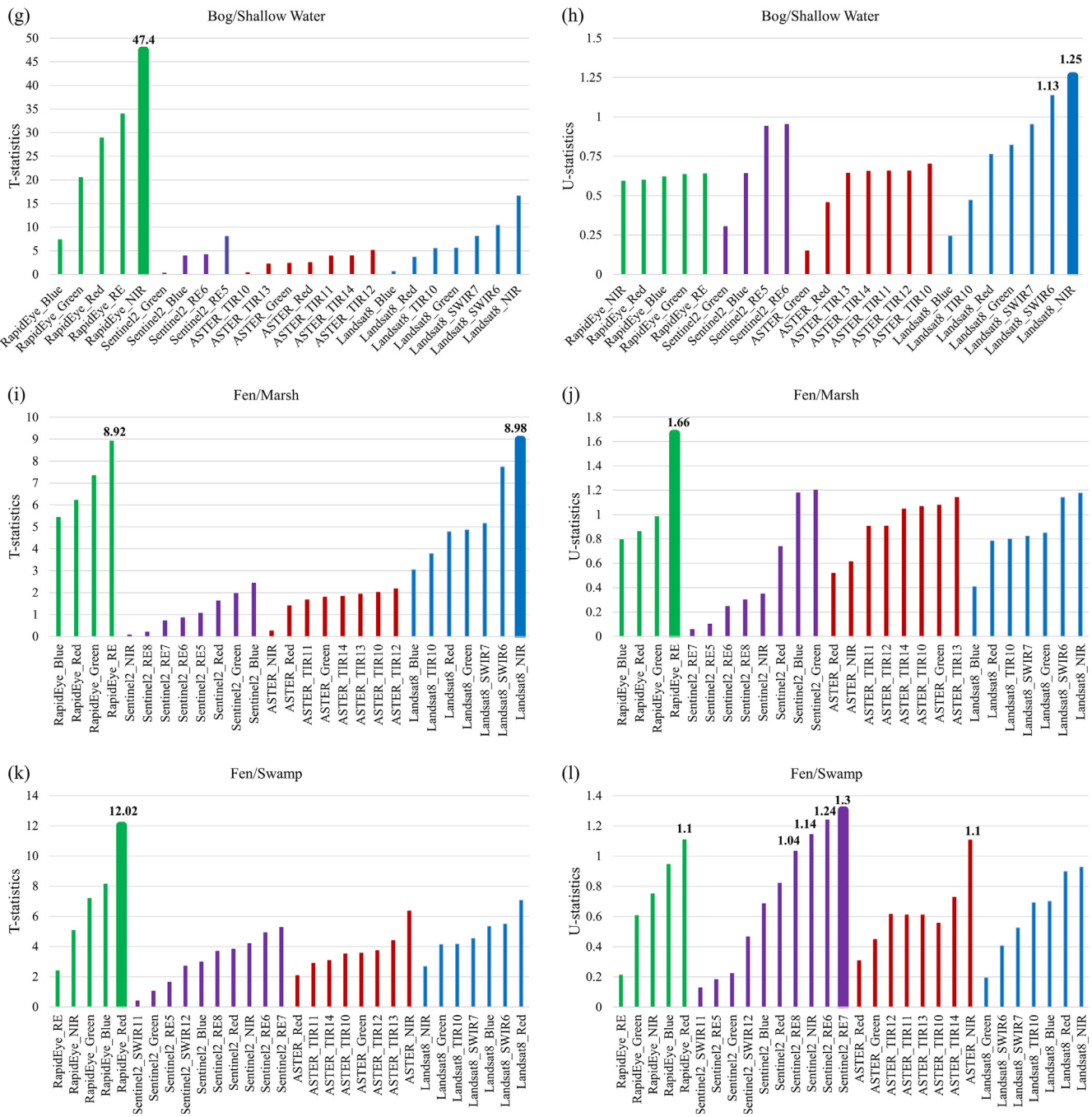


Fig. 3. (continued)

3.5. Wetland classification using selected features

After performing the separability analyses of the spectral bands and the features listed in Table 6, the selected features were injected into an object-based RF classifier to obtain wetland maps of the study areas. The RF algorithm was selected because it performed better than other classifiers based on our previous studies (Amani et al., 2017b,c; Mahdavi et al., 2017a). RF has also been successful in many studies of classification of vegetation and complex environments, such as wetlands (Adam et al. 2010; Mutanga et al., 2012; Mahdianpari et al., 2017). Moreover, one of the benefits of using the RF classifier is that various data sources from different measurement scales can be easily incorporated into the classification (Adam et al., 2010). Since all the images used in this study had medium spatial resolution, the object-based method was used instead of the traditional pixel-based method.

The multi-resolution algorithm was first used to segment the image using the spectral and spatial information and, then, the classification is performed on the objects as the minimum unit of analysis (Duro et al., 2012). Both segmentation and classification were performed in eCognition™ 9 software (Definiens, 2009). It is worth noting that both RF and multi-resolution algorithms contain different input parameters, which should be carefully selected to obtain a high classification accuracy. This matter is discussed in more details in our previous study (see Amani et al., 2017b).

4. Results and discussion

4.1. Variance analyses of field samples

As mentioned in Section 3.1, Eq. (1) was used for variance analysis

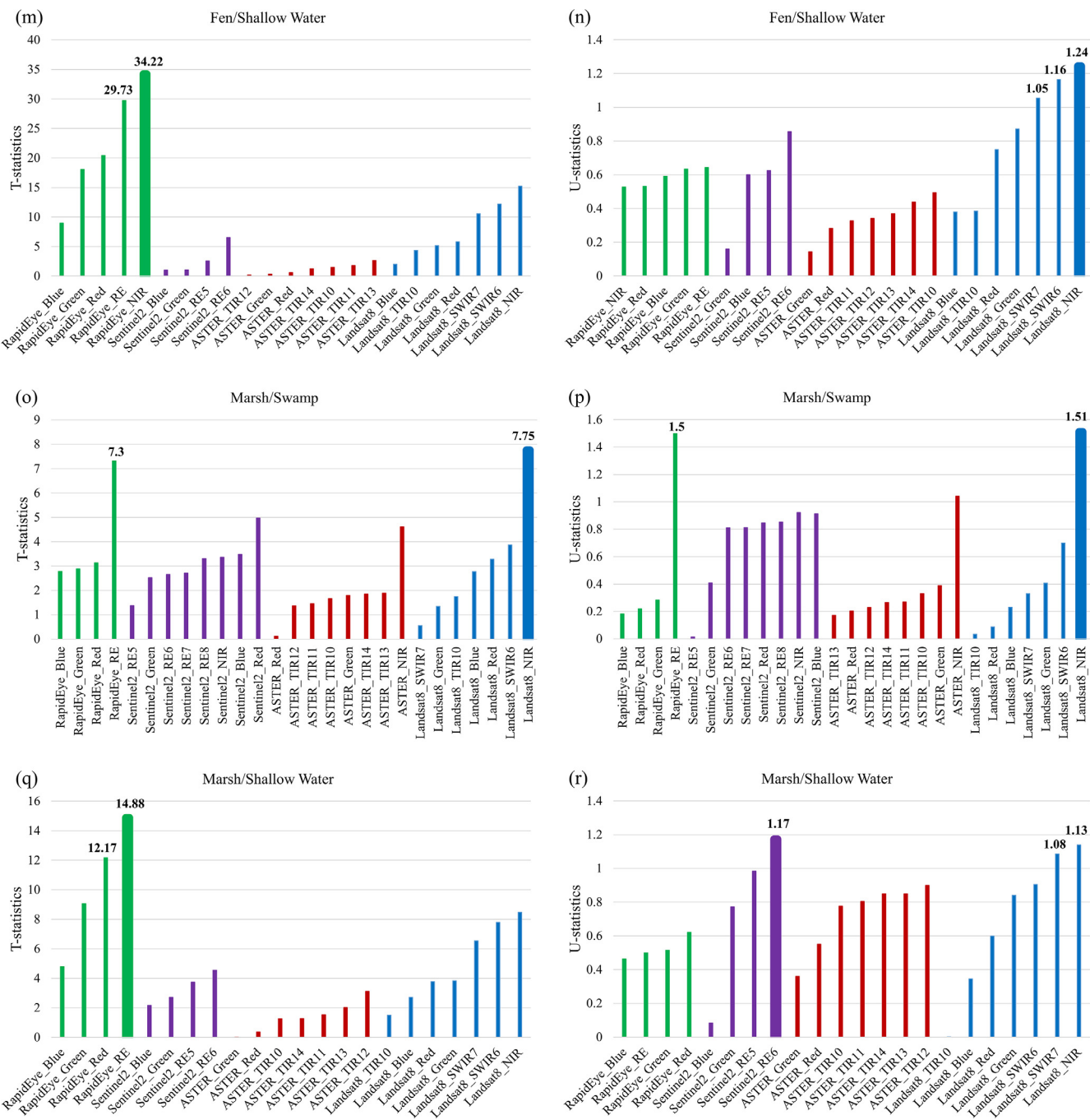


Fig. 3. (continued)

of field samples and only the spectral bands for which the corresponding field samples had relatively similar reflectance values (lower variance) were used for the next experiments (see Fig. 2(a) as an example). Fig. 2(b) illustrates a spectral band, for which the variation of reflectance values of field samples was high and, therefore, the band was removed from the next analyses. According to Table 5, there were 30 spectral bands extracted from four different optical sensors, from which the spectral responses of five wetland types were analyzed. Consequently, there were $30 \times 5 = 150$ features extracted from the images. Finally, 10 features were removed from the subsequent experiments based on variance values calculated from Eq. (1).

After performing variance analyses on the individual wetland classes, variance analyses on wetland class pairs were then performed using the F-test statistics (Eq. (2)). In this step, 13 features were removed from the next experiments. Finally, an attempt was made to

select the best features (out of 127 remaining features) to classify wetlands using separability analyses, which are discussed in more detail in the next three subsections.

4.2. Separability analyses of spectral bands

Fig. 3 illustrates the amount of separability between different wetland class pairs in various spectral bands, which was obtained using two measures: T-statistics and U-statistics. Based on the values of the T-statistics and U-statistics illustrated in Fig. 3, the most useful spectral bands for distinguishing the different pairs of wetland types are also summarized in Table 7. As evident from this table, only one band is recommended for separating some pairs, however, multiple spectral bands are recommended for separating others. The separability of wetlands is also visualized by plotting the spectral signatures of the

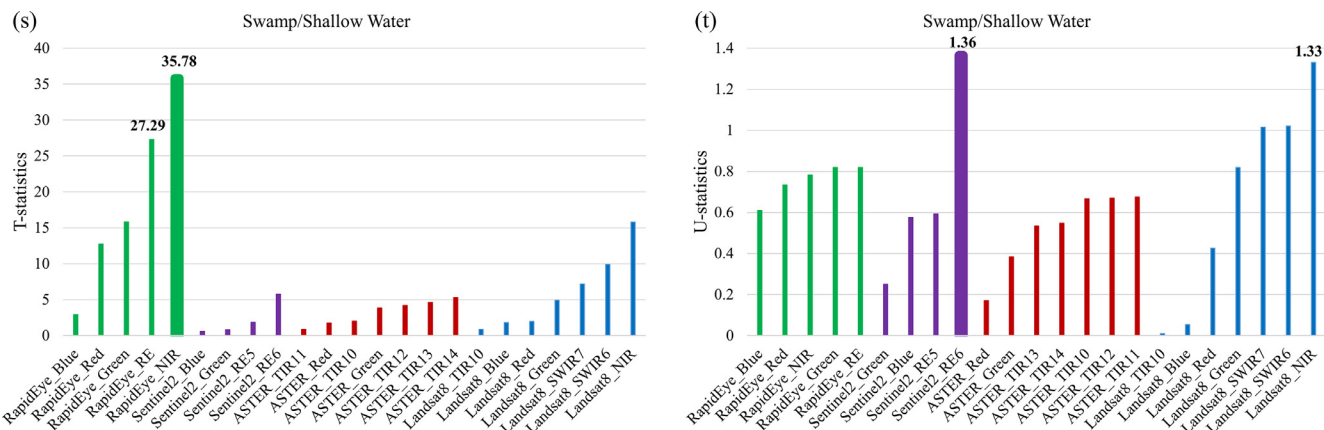


Fig. 3. (continued)

Table 7

The most useful spectral bands for discriminating between each pair of wetland classes in late spring (June) using two distance measures. The spectral bands are ordered based on their separability measures (the spectral bands indicated in the upper right half of the table and the lower left half of the table were obtained using the T-statistics and U-statistics, respectively).

	Bog	Fen	Marsh	Swamp	Shallow Water
Bog	×	Landsat8 NIR RapidEye RE RapidEye NIR	Landsat8 NIR RapidEye RE RapidEye NIR	RapidEye Red	RapidEye NIR
Fen	Sentinel2 RE5 Landsat8 NIR Sentinel2 NIR	×	Landsat8 NIR RapidEye RE	RapidEye Red	RapidEye NIR RapidEye RE
Marsh	Landsat8 NIR RapidEye RE Sentinel2 RE5	RapidEye RE	×	Landsat8 NIR RapidEye RE	RapidEye RE RapidEye Red
Swamp	Landsat8 Red	Sentinel2 RE7 Sentinel2 RE6 Sentinel2 NIR ASTER NIR RapidEye Red Sentinel2 RE8	Landsat8 NIR RapidEye RE	×	RapidEye NIR RapidEye RE
Shallow Water	Landsat8 NIR Landsat8 SWIR6	Landsat8 NIR Landsat8 SWIR6 Landsat8 SWIR7	Sentinel2 RE6 Landsat8 NIR Landsat8 SWIR7	Sentinel2 RE6 Landsat8 NIR	×

classes in Fig. 4.

As clear from Fig. 3 and Table 7, the results obtained by the T-test and U-test were not always consistent. This was expected as each of these methods considers different assumptions for samples distribution. However, both separability methods were considered in this study to obtain a comprehensive conclusion. It should be noted that the results obtained by the U-test were more trustful compared to the T-test in this study because the variance values of field wetland samples were considerably high (see Section 3.1) and the data did not generally follow a normal distribution. Finally, the following results were obtained by considering the results of both distance measures.

The NIR band was the most useful spectral band for discriminating wetland classes. The NIR band is the most important band for vegetation studies, and is a useful band to study the biomass content of vegetation and its health. The NIR band is also helpful in distinguishing water bodies from land because water strongly absorbs the NIR light, while soil and vegetation reflects more energy in this region of spectrum (Schmidt and Skidmore, 2003; Manevski et al., 2011). Consequently, the NIR band is often the most helpful spectral bands in wetland studies, for which vegetation and water are two important components. For example, in all cases except for Bog/Swamp, Fen/Swamp, and Marsh/Shallow Water, the NIR band was the best band to discriminate wetland class pairs (see Fig. 3 and Table 7). According to Fig. 3, the Landsat 8 NIR band produced the largest separability for wetland class pairs in 6 out of 10 cases. The results obtained from the

spectral signatures (Fig. 4) also supported these results, where the greatest variation was observed in the NIR bands. It is also worth noting that this difference was most significant for the Shallow Water class.

The RE bands produced the second best discrimination between wetland class pairs, as well as all wetland classes. The RE band provides valuable information about both biochemical and biophysical parameters of wetlands, such as chlorophyll content and the Leaf Area Index (LAI). This band is also useful in assessing the water deficit in wetland biomass (Filella and Penuelas, 1994; Mutanga and Skidmore, 2007). Moreover, the RE band has been widely used to monitor vegetation growth and, thus, was very useful for distinguishing wetlands, which are highly dynamic environments. For instance, in 5 out of 10 cases, the RE bands of the RapidEye and/or Sentinel 2A were selected as the best spectral bands using either the T-statistics or U-statistics in separating wetland type pairs (Fig. 3). The RE bands were also among the best spectral bands to discriminate the Marsh class from other wetland classes using both the T-statistics and U-statistics (see Table 7). Moreover, more variation in the response of wetland classes was observed in the RE bands compared to that of the SWIR, TIR, and visible bands (Fig. 4).

Comparing the visible bands, the red band had the strongest power to delineate the wetland classes. The red band is useful in studies of vegetation, soil types, and geology. This spectral band is mostly used for detecting chlorophyll absorption in vegetation, as well as for evaluating the composite of the soil, where soils with rich iron-oxide have a high

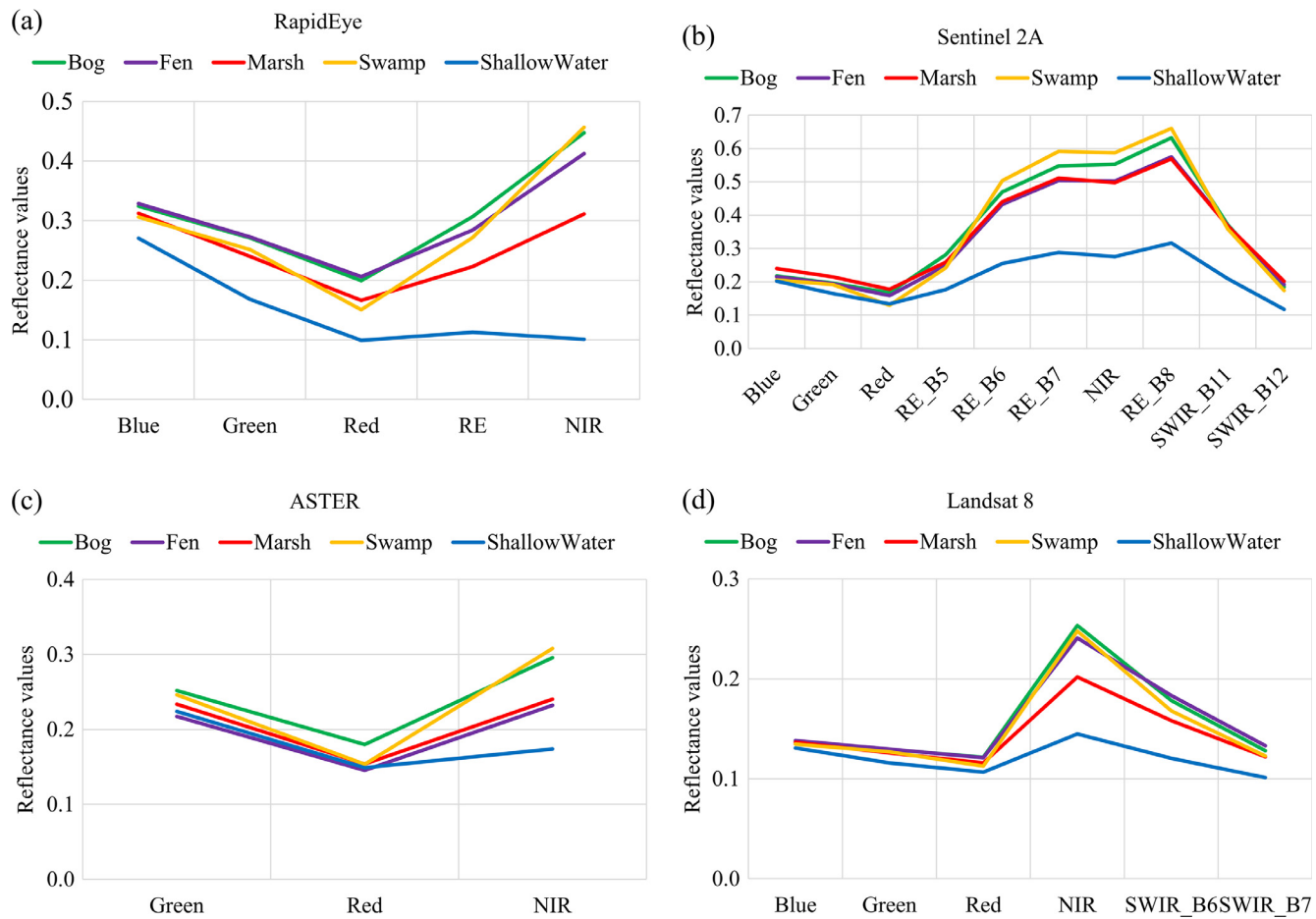


Fig. 4. The spectral signature of wetlands, obtained from (a) RapidEye, (b) Sentinel 2A, (c) ASTER, and (d) Landsat 8.



Fig. 5. The red/orange appearance of bogs in the study areas. (For interpretation of the references to colour in this figure legend, the reader is referred to the web version of this article.)

reflectance in this band (Schmidt and Skidmore, 2003; Manevski et al., 2011). Therefore, this band was very helpful for discriminating several wetlands, which contain different types of soils and vegetation with various amounts of chlorophyll content. For instance, according to the spectral signatures obtained from different satellites (Fig. 4), bog wetlands reflected greater energy in the red band compared to the other wetland classes. The reason may be that bog wetlands in NL contain more sphagnum moss, which often has a red or orange appearance (see Fig. 5). Note the red appearance of bog due to the presence of red sphagnum moss). As a consequence, this band was one of the best spectral bands to distinguish the Bog class from other wetland classes (see Fig. 3(e and f) as examples). In addition, the spectral signatures of wetlands obtained from the RapidEye and ASTER data also presented some differences between mean values of the Bog class from the other

wetland classes in the red band (Fig. 4). It is also worth mentioning that the red band has been used in distinguishing between vegetation and man-made objects (Shettigara et al., 1995), and it was expected to be useful in delineating wetlands from urban areas.

The SWIR bands exhibited intermediate separability, and were helpful in some cases (e.g. for discriminating the Shallow Water class from other wetland classes). The SWIR band is sensitive to the moisture content in soil and vegetation. The reflectance in this band decreases as moisture content increases. This is helpful for discriminating wet from dry land covers (Crist and Cicone, 1984). However, since all types of wetlands are generally wet, this spectral band was not as informative as the NIR and RE bands. As expected, this band is more useful for discriminating between wetlands and uplands.

The green band is also useful in assessing plant vigor, as well as in

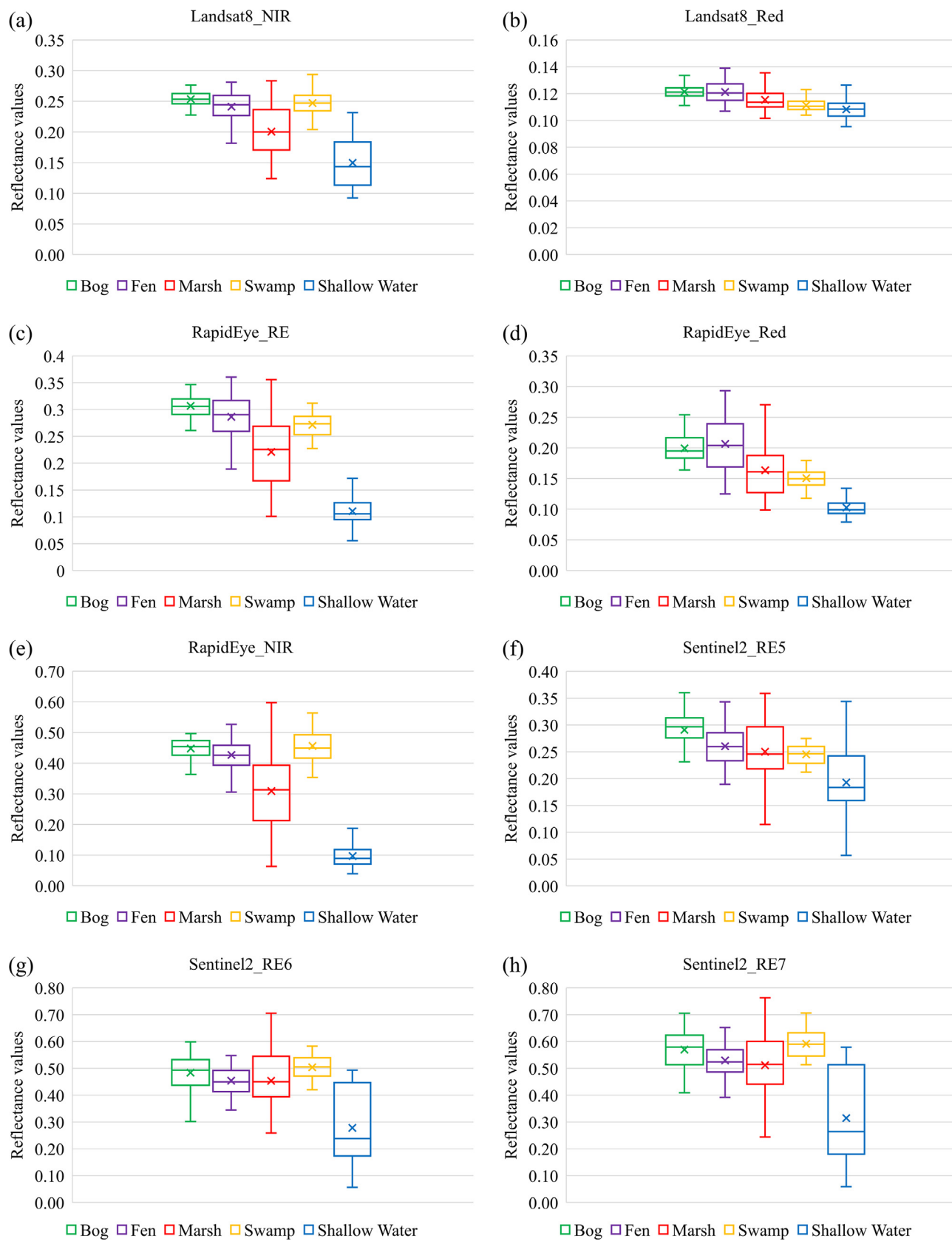


Fig. 6. The box plots of the spectral bands, which provided the highest separability for wetland classes in late spring (June). The cross (\times) mark indicates the mean value. The numbers after the name of the spectral bands indicate the number of the band. For example: Sentinel2_RE6 is the Red Edge band (band 6) of Sentinel 2A. (For interpretation of the references to colour in this figure legend, the reader is referred to the web version of this article.)

Table 8

The best features for separating different wetland class pairs based on two separability measures: T-statistics and U-statistics.

T-test		U-test	
Feature	T-statistics	Feature	U-statistics
<i>Bog/Fen</i>			
RapidEye RE Ratio	11.12	ASTER Green Ratio	2.79
Landsat8 SWIR7 Ratio	8.62	ASTER NDWI	2.44
Landsat8 NIR Ratio	8.18	RapidEye RE Ratio	2.10
RapidEye Green Ratio	7.78	Sentinel2 SWIR12 Ratio	1.88
Landsat8 NDSI6	7.25	Landsat8 NIR Ratio	1.87
RapidEye Blue Ratio	7.12	Sentinel2 Green Ratio	1.84
RapidEye NDVI	7.01	ASTER Red Ratio	1.82
RapidEye NIR Ratio	6.91	Sentinel2 NDWI	1.74
RapidEye_NIR	6.78	Sentinel2 Blue Ratio	1.69
Landsat8 NDSI7	6.64	Mean Landsat8 NIR	1.63
<i>Bog/Marsh</i>			
RapidEye RE Ratio	16.19	ASTER Green Ratio	3.14
RapidEye Green Ratio	15.57	ASTER NDWI	2.83
Landsat8 DVI	13.89	Sentinel2 Green Ratio	1.96
Landsat8 NIR	13.74	Sentinel2 NDWI	1.89
RapidEye RE	13.66	ASTER Red Ratio	1.85
Landsat8 NDSI7	13.47	RapidEye Green Ratio	1.73
Landsat8 NIR Ratio	12.74	Sentinel2 NDSI12	1.68
RapidEye NIR	12.37	Landsat8 NIR	1.54
RapidEye DVI	12.34	RapidEye RE Ratio	1.53
Landsat8 SAVI	12.14	Landsat8 NDWI	1.53
<i>Bog/ Swamp</i>			
RapidEye Red	19.9	Sentinel2 SAVI	2.04
RapidEye Red Ratio	17.5	Sentinel2 RE5 NDVI	2.02
RapidEye NDVI	14.47	Landsat8 Green Ratio	2.00
RapidEye RE NDVI	14.25	ASTER SAVI	1.95
RapidEye RE Ratio	14.22	Landsat8 Blue Ratio	1.93
RapidEye SAVI	13.43	ASTER DVI	1.89
RapidEye RE	13.24	Sentinel2 NDVI	1.89
RapidEye Blue	11.25	Sentinel2 RE6 Ratio	1.89
RapidEye NIR Ratio	11.09	Landsat8 NDVI	1.86
RapidEye Brightness	10.02	ASTER NDVI	1.80
<i>Bog/Shallow water</i>			
RapidEye NIR	48.42	ASTER Green Ratio	2.56
RapidEye DVI	43.28	RapidEye Green Ratio	2.31
RapidEye RE	33.30	ASTER NDWI	2.05
RapidEye Brightness	32.54	RapidEye NIR Ratio	1.99
RapidEye NIR Ratio	31.58	RapidEye RE Ratio	1.97
RapidEye RE Ratio	26.76	Sentinel2 NDWI	1.89
RapidEye NDWI	26.22	Sentinel2 Green Ratio	1.84
RapidEye Red	24.89	Sentinel2 Red Ratio	1.81
RapidEye Green Ratio	23.79	Sentinel2 NDSI12	1.81
RapidEye NDVI	21.38	Sentinel2 Blue Ratio	1.75
<i>Fen/Marsh</i>			
Landsat8 NIR	10.32	ASTER NIR Ratio	2.15
Landsat8 Blue Ratio	10.14	Sentinel2 Green Ratio	1.94
RapidEye Brightness	9.61	RapidEye Blue Ratio	1.80
Landsat8 NDWI	9.35	RapidEye Green Ratio	1.79
Landsat8 DVI	9.31	Sentinel2 NDWI	1.76
RapidEye Blue Ratio	8.77	ASTER NDVI	1.75
Landsat8 Brightness	8.59	ASTER DVI	1.697
RapidEye RE Ratio	8.58	ASTER SAVI	1.69
RapidEye NIR Ratio	8.46	Standard deviation	1.69
Landsat8 NDVI	8.31	RapidEye NDWI	1.66
<i>Fen/ Swamp</i>			
RapidEye NDVI	14.02	Landsat8 NIR Ratio	2.16
RapidEye Red Ratio	13.91	ASTER Red Ratio	2.01
RapidEye SAVI	13.07	ASTER NDWI	1.86
RapidEye NDWI	12.70	Landsat8 SAVI	1.85
RapidEye Red	11.75	Landsat8 NDVI	1.85
RapidEye NIR Ratio	11.60	ASTER Green Ratio	1.75
RapidEye RE6 NDVI	11.31	RapidEye NDVI	1.70
RapidEye Blue	10.95	Landsat8 DVI	1.67
RapidEye DVI	9.98	Sentinel2 NDVI	1.65
Standard deviation	9.54	RapidEye DVI	1.64
RapidEye Red			

Table 8 (continued)

T-test	U-test		
Feature	T-statistics	Feature	U-statistics
<i>Fen/Shallow Water</i>			
RapidEye NIR	31.39	RapidEye NDWI	2.47
RapidEye RE	26.78	RapidEye Blue Ratio	2.16
RapidEye Brightness	26.64	RapidEye Green Ratio	2.08
RapidEye DVI	26.52	Sentinel2 NDWI	2.08
RapidEye RE Ratio	26.25	Sentinel2 RE5 Ratio	1.93
RapidEye NIR Ratio	23.503	Sentinel2 Blue Ratio	1.90
RapidEye Green Ratio	22.37	Sentinel2 Red Ratio	1.86
RapidEye NDWI	21.50	ASTER NIR Ratio	1.82
RapidEye RE NDVI	20.61	Sentinel2 Green Ratio	1.77
RapidEye Green	19.64	ASTER DVI	1.74
<i>Marsh/ Swamp</i>			
RapidEye NDVI	16.65	Landsat8 SAVI	1.87
RapidEye DVI	15.36	Landsat8 NDVI	1.81
RapidEye SAVI	15.18	Sentinel2 SAVI	1.81
RapidEye RE NDVI	13.71	Landsat8 NIR Ratio	1.77
RapidEye Red Ratio	13.16	Landsat8 DVI	1.68
Landsat8 DVI	13.02	Landsat8 NIR	1.68
Landsat8 NDWI	12.96	ASTER DVI	1.62
RapidEye NDWI	12.66	Sentinel2 RE7 Ratio	1.60
RapidEye NIR Ratio	12.37	ASTER SAVI	1.59
Landsat8 Red Ratio	11.99	Sentinel2 RE6 Ratio	1.55
<i>Marsh/Shallow water</i>			
RapidEye Blue Ratio	16.94	RapidEye RE Ratio	2.45
RapidEye RE NDVI	16.38	RapidEye Green Ratio	2.15
RapidEye Brightness	15.57	RapidEye NDWI	2.07
RapidEye NIR	15.12	Sentinel2 Red Ratio	1.98
RapidEye NDWI	14.83	Sentinel2 RE5 Ratio	1.95
RapidEye NIR Ratio	14.57	Sentinel2 NDWI	1.94
RapidEye RE	14.12	Landsat8 Blue Ratio	1.87
RapidEye DVI	14.12	Sentinel2 Blue Ratio	1.75
RapidEye Red	12.827	Landsat8 NDWI	1.65
Standard deviation	12.64	Sentinel2 Green Ratio	1.64
RapidEye NIR			
<i>Swamp/Shallow water</i>			
RapidEye NIR	38.74	RapidEye Blue Ratio	1.84
RapidEye DVI	35.49	ASTER Green Ratio	1.68
RapidEye NIR Ratio	33.20	Sentinel2 NDWI	1.65
RapidEye RE Ratio	27.79	RapidEye Green Ratio	1.63
RapidEye Brightness	26.81	Sentinel2 Green Ratio	1.62
RapidEye RE NDVI	26.65	RapidEye NDWI	1.58
RapidEye NDWI	26.61	RapidEye Red Ratio	1.57
RapidEye RE	26.26	Landsat8 DVI	1.53
RapidEye NDVI	25.51	ASTER DVI	1.51
RapidEye SAVI	23.61	Sentinel2 Red Ratio	1.47

isolating different types of vegetation, where healthy and green vegetation reflects more energy in this region (Adam et al., 2010). Although the green bands were not selected as the best spectral bands in Table 7, they were more appropriate for distinguishing wetland class pairs (Fig. 3), as well as all wetland classes compared to the blue and TIR bands.

Although several studies have argued that the TIR bands had potential for the separability of water bodies from wetland vegetation (e.g. Leblanc et al., 2011; Amani et al., 2017a), this band was not as helpful as the other spectral bands for separating various wetland classes. One main reason for this result may be due to the coarse spatial resolution of TIR bands in satellite data compared to the other spectral bands resulting in mixed pixels.

In addition, the result of the analyses in this study indicated that the pairs of wetland classes were more difficult to distinguish in the blue band, in which wetland classes were spectrally similar. For instance, as demonstrated in Fig. 4, the highest overlap in the spectral signatures of wetlands was observed in the blue band of the satellites.

In addition, the following results were obtained based on the analyses of the spectral signatures of the wetland classes (Fig. 4):

Table 9

The best features for wetland classification in the study areas.

Feature	Frequency
RapidEye NIR Ratio	13
RapidEye RE Ratio	11
RapidEye NDWI	10
Landsat8 Green Ratio	9
RapidEye DVI	8
RapidEye NDVI	7
RapidEye NIR Ratio	7
Sentinel2 Green Ratio	7
Sentinel2 NDWI	7
Landsat8 DVI	6
RapidEye Brightness	6
RapidEye NIR	6
RapidEye RE	6
RapidEye RE NDVI	6
RapidEye Blue Ratio	6
ASTER DVI	5
ASTER Green Ratio	5
Landsat8 NIR	5
ASTER NDWI	4
Landsat8 NDVI	4
Landsat8 NDWI	4
RapidEye Red	4
RapidEye Red Ratio	4
RapidEye SAVI	4
Sentinel2 Blue Ratio	4
Sentinel2 Red Ratio	4
ASTER Red Ratio	3
ASTER SAVI	3
Landsat8 Blue Ratio	3
Landsat8 SAVI	3
ASTER NDVI	2
ASTER NIR Ratio	2
Landsat8 NDSI7	2
RapidEye Blue	2
Sentinel2 NDSI12	2
Sentinel2 NDVI	2
Sentinel2 RE5 Ratio	2
Sentinel2 RE6 Ratio	2
Sentinel2 SAVI	2
Landsat8 Brightness	1
Landsat8 Green Ratio	1
Landsat8 NDSI6	1
Landsat8 Red Ratio	1
Landsat8 SWIR7 Ratio	1
RapidEye Green	1
RapidEye NIR (Standard deviation)	1
Sentinel2 RE5 NDVI	1
Sentinel2 RE7 Ratio	1
RapidEye Red (Standard deviation)	1
Sentinel2 RE5 (Standard deviation)	1

- (1) The spectral signatures of vegetated wetlands (i.e. Bog, Fen, Marsh, and Swamp) followed the same patterns, and were similar to the spectral signatures of green vegetation, for which the highest and lowest values were observed in the NIR and red bands, respectively.
- (2) The spectral signatures of the Shallow Water class were not completely similar to the spectral signature of clean and open water. In fact, in some cases, the NIR values of the Shallow Water class were more than that of the visible bands. This can be explained by the fact that there were some aquatics beds with emergent vegetation in and on the shallow water bodies in the study areas.
- (3) The Shallow Water class was spectrally distinct from other wetland classes in all spectral bands.
- (4) The Shallow Water and Bog classes generally had the lowest and highest responses, respectively.
- (5) Compared to the other vegetated wetlands, the Marsh class presented the lowest spectral response in almost all spectral bands. This was because, generally, the Marsh class contains more open water than other vegetated wetland classes found in the study areas.

Fig. 6 illustrates the distribution of the reflectance values for the wetland classes in the most effective spectral bands (see **Table 7**) using boxplots. Different wetland classes had similar reflectance values in the spectral bands, making the separation of complex wetlands a challenging task. This is also supported by the spectral signatures of the wetland classes (**Fig. 4**), where there was considerable overlap between the values of wetland classes, especially between the vegetated wetland types.

Additionally, according to **Fig. 6**, high variance was observed for some wetland classes, such as the Marsh and Shallow Water classes. This can be attributed to the fact that each of these wetland classes contained more than one land cover type, as described in the EWCS (Smith et al., 2007). For instance, the Marsh and Shallow Water classes contain both vegetation and water (i.e. meadow/emergent marsh and aquatic bed/open water) and, therefore, their spectral responses were affected by both vegetation and water.

Based on the results, it is suggested to select those satellites for wetland classification that contain the NIR and RE bands. For instance, Sentinel 2A, which contains four different RE bands can be one of the most useful optical satellites in this regard. However, the spatial resolution of the satellite data is also important, especially when OBIA is applied to classify wetlands. Thus, RapidEye with 5 m spatial resolution and both the RE and NIR bands also provide valuable data for wetland studies. Additionally, the temporal resolution of optical satellites is important for dynamic wetland environments and, therefore, Sentinel 2A and RapidEye with approximately 5 days revisit time are more suitable than Landsat 8 and ASTER with 16 days temporal resolution.

4.3. Separability analyses of other features

It is clear that even with the best spectral bands, it was difficult to delineate the wetland classes. Therefore, in this subsection, other features are evaluated to ameliorate this task. All of the steps performed for selecting the best spectral bands (obtained from the mean reflectance values of the field samples) were performed for several other features, including spectral indices, texture and ratio features (see **Table 6**).

The variance analyses primarily showed that the brightness, mean and ratio values had the lowest variations and, therefore, the corresponding features were most reliable for wetland classification in the study areas. On the other hand, the highest variance in the values of field samples was observed for the standard deviation features and, thus, the corresponding features were removed from the rest of the analyses.

After performing variance analyses, the distance between the pairs of wetland classes was calculated using the T- and U-statistics and the best features, providing the highest separability were obtained (**Table 8**). Moreover, **Table 9** demonstrates the spectral bands and features that provided the maximum spectral separation between all wetland classes, obtained from aggregating the results provided in **Table 8**. The frequency in **Table 9** indicates how many times a spectral band or a feature was selected as the best feature for discriminating wetland pairs.

The ratio features were generally the most helpful features for discriminating wetland pairs. In this regard, the highest T- and U-statistics were obtained for the NIR, RE, Green, and Red ratios, respectively. It can also be seen from **Table 9** that the wetland classes had greater potential of being separable using the RapidEye NIR and RE ratios and, thus, they were selected as the best features for 13, and 11 times, respectively.

The selected spectral indices were also helpful in discriminating different pairs of wetland classes. The Normalized Difference Water Index (NDWI), Normalized Difference Vegetation Index (NDVI), Difference Vegetation Index (DVI), and Soil Adjusted Vegetation index (SAVI) were the best spectral indices, respectively. However, the Normalized Difference Soil Index (NDSI) was not as good as the other

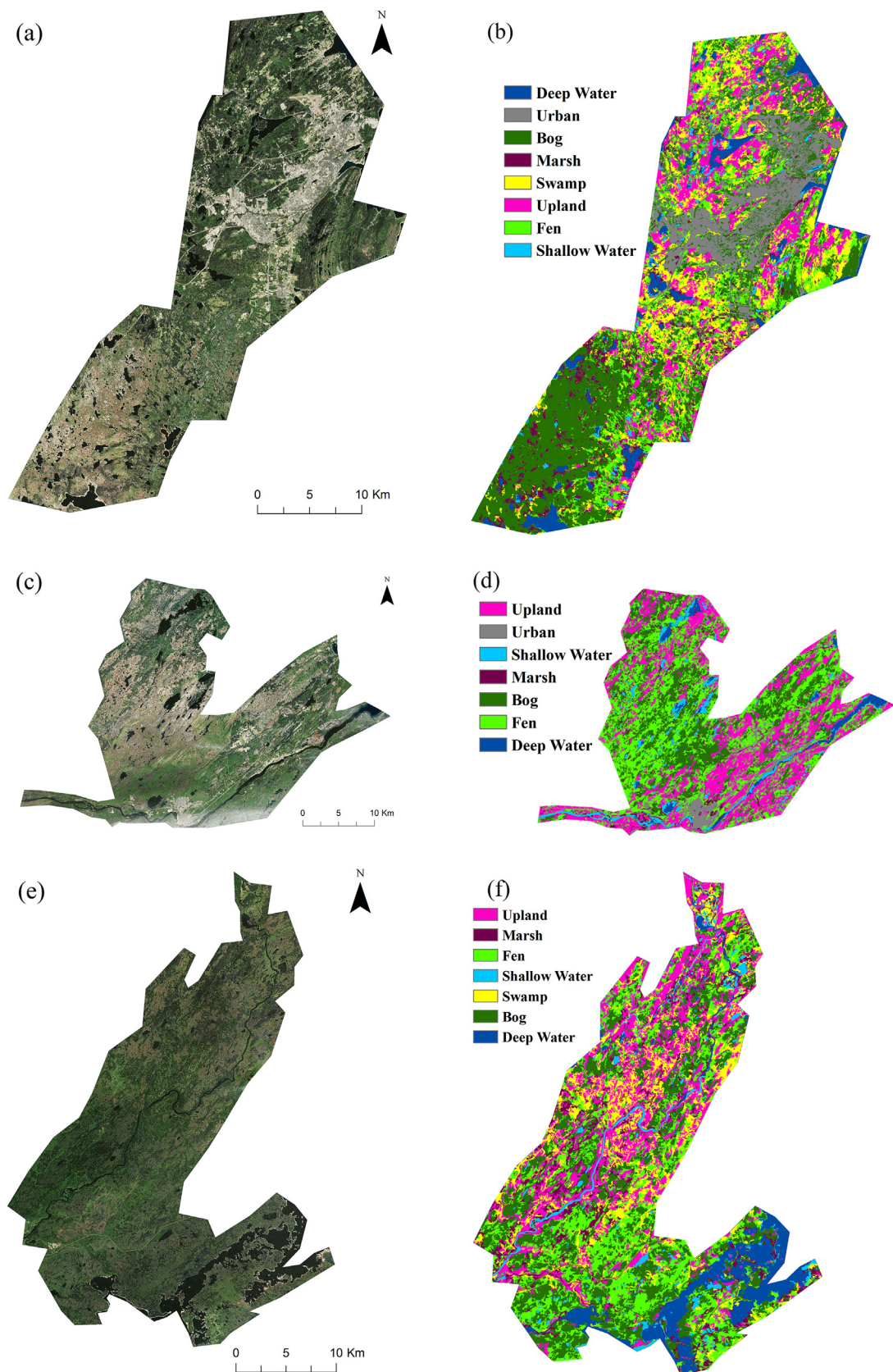


Fig. 7. The study areas and their corresponding classified maps.

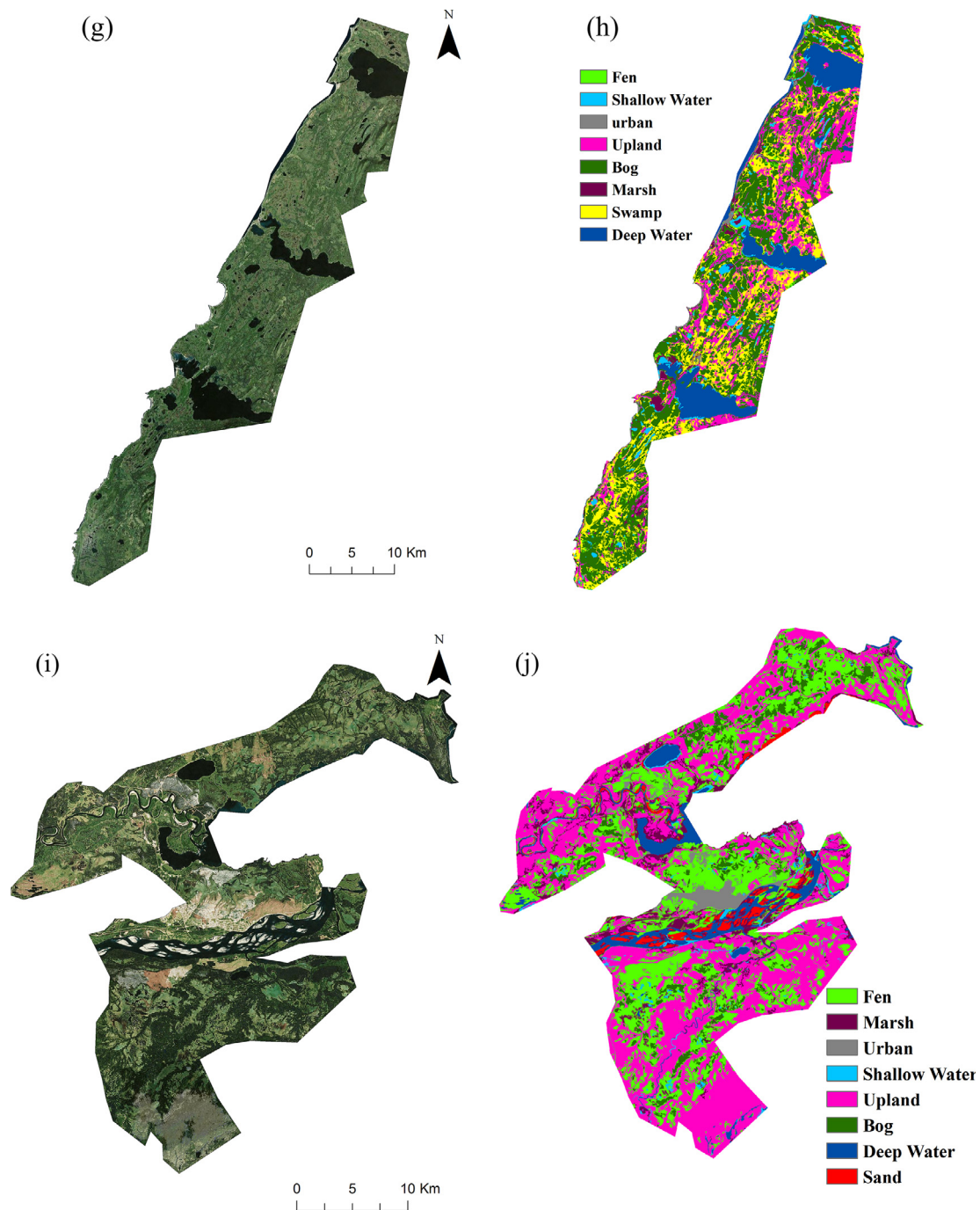


Fig. 7. (continued)

spectral indices. The reason was the NDSI considers the SWIR band, which was not as helpful as the other spectral bands (see previous subsection).

Additionally, the best spectral bands, selected in the previous subsection, were between the most useful features for discrimination wetland class pairs in this section. For example, either the NIR and RE bands were selected as one of the best features for distinguishing the wetland class pairs.

4.4. Wetlands classification using selected features

After selecting the best features for separating different wetland classes, they were injected into an object-based RF algorithm to obtain wetland maps from the study areas. To do this, half of the field samples

was randomly used to train the algorithm and the other half was applied to evaluate the classification accuracy. Fig. 7 illustrates the classified wetland maps.

Based on the visual interpretation, which has been carried out by several ecological and RS experts using aerial imagery (pixel size = 0.5 m) and the ground truth data, it was concluded that all classes in most regions of the study areas were generally classified well. For example, according to the field measurements, the south of the Avalon study area, which is mostly covered by bogs, fens, and marshes, was correctly mapped in the classified image. Additionally, the areas surrounding deep waters, as well as the small water bodies, were classified as Shallow Water, which indicated that these regions were classified accurately. It was also concluded that the urban and deep water areas in most parts of the study areas have been identified

Table 10

The OA, Kappa coefficient, Mean PA and UA of wetland classes in the five study areas.

	Avalon	Grand Falls-Windsor	Deer Lake	Gros Morne	Goose Bay
OA (%)	88	84	82	89	86
Kappa coefficient	0.85	0.81	0.75	0.85	0.83
Mean PA of wetland classes (%)	75	68	73	71	76
Mean UA of wetland classes (%)	78	72	69	75	74

correctly. The OAs, Kappa coefficients, and mean PAs and UAs for wetland classes in each study area are also provided in Table 10. According to the levels of classification accuracies, it was concluded that the selected features in previous subsections had a high potential for the separation of different wetland classes in this study providing the accuracies more than 80%.

5. Conclusion

The mapping and monitoring of wetlands using new technologies are important because they provide many beneficial services to both the environment and humans. In this regard, optical RS satellites provide valuable data. One main concern in utilizing the optical data is finding the most informative bands and features for delineation of various wetland types. For this purpose, and to have a reliable and robust approach, the data acquired by four different optical satellites, including RapidEye, Sentinel 2A, ASTER, and Landsat 8 were investigated. Variance analyses should be carried out on the field data collected for wetland studies before performing any separability analysis. This is because wetlands are dynamic and complex environments and one wetland type can contain various land covers. Consequently, the spectral responses of the field samples of one particular wetland class can vary considerably. This fact is more important when using textural features (e.g. standard deviation values of field sample polygons), as there were high variances in their values and, thus, should be eliminated from the analyses. According to the spectral analyses, it was concluded that generally the NIR, RE, and red bands were the most useful spectral bands for the differentiation of wetland species, respectively. Thus, the corresponding ratio features and the spectral indices, derived from these bands (e.g. NDWI and NDVI) were among the best features for wetland classification. Additionally, these results demonstrated that the data acquired by some optical satellites, such as RapidEye and Sentinel 2A, which contain both NIR and RE bands may be the most appropriate for achieving high accuracy in wetland classifications. It was also concluded that the spectral responses of vegetated wetlands (i.e. Bog, Fen, Marsh, and Swamp) were very similar in some spectral bands and there were difficulties in discriminating them. Use of multi-temporal data or other types of RS data, such as SAR, might solve this problem. For instance, SAR data demonstrate a high potential for soil moisture estimation which is one of the main characteristics of wetlands. Thus, the separability analyses of wetlands should also be carried out using different types of SAR data to select the most useful SAR features to differentiate wetlands. Furthermore, since wetlands are highly changeable over time (i.e. seasonally or even monthly), similar spectral analyses, performed in this study for the data captured in June, is suggested to be carried out using the satellite data acquired in other times to obtain a more versatile conclusion regarding the best spectral features for delineation of wetland classes. Finally, after selecting the most useful features for the delineation of wetland classes, they were used in an object-based RF algorithm to classify the

wetlands in five different study areas. It was concluded that the selected spectral bands and features had a high potential for monitoring wetlands over various regions of NL.

Acknowledgement

This project was undertaken with the financial support of the Government of Canada through the Federal Department of Environment and Climate Change. Field data was collected by various organizations including, Ducks Unlimited Canada, Government of Newfoundland and Labrador Department of Environment and Conservation, and Nature Conservancy Canada. The authors thank these organizations for the generous financial supports and providing such valuable datasets. The authors also would like to appreciate Ms. Jean Granger's great effort in collecting and preparing the field data.

References

- Adam, E., Mutanga, O., 2009. Spectral discrimination of papyrus vegetation (*Cyperus papyrus* L.) in swamp wetlands using field spectrometry. *ISPRS J. Photogramm. Remote Sens.* 64 (6), 612–620.
- Adam, E., Mutanga, O., Rugege, D., 2010. Multispectral and hyperspectral remote sensing for identification and mapping of wetland vegetation: a review. *Wetlands Ecol. Manage.* 18 (3), 281–296.
- Amani, M., Salehi, B., Mahdavi, S., Granger, J., 2017. Spectral analysis of wetlands in Newfoundland using Sentinel 2A and Landsat 8 imagery. In: IGFT 2017, ASPRS Annual Conference.
- Amani, M., Salehi, B., Mahdavi, S., Granger, J.E., Brisco, B., Hanson, A., 2017b. Wetland classification using multi-source and multi-temporal optical remote sensing data in Newfoundland and Labrador, Canada. *Can. J. Remote Sens.* 1–14.
- Amani, M., Salehi, B., Mahdavi, S., Granger, J., Brisco, B., 2017c. Wetland classification in Newfoundland and Labrador using multi-source SAR and optical data integration. *GIScience Remote Sens.* 1–18.
- Araya-López, R.A., Lopatin, J., Fassnacht, F.E., Hernández, H.J., 2018. Monitoring Andean high altitude wetlands in central Chile with seasonal optical data: a comparison between Worldview-2 and Sentinel-2 imagery. *ISPRS J. Photogramm. Remote Sens.*
- Chatziantoniou, A., Psomiadis, E., Petropoulos, G.P., 2017. Co-Orbital Sentinel 1 and 2 for LULC mapping with emphasis on wetlands in a mediterranean setting based on machine learning. *Remote Sensing* 9 (12), 1259.
- Conover, W.J., 1980. Practical Nonparametric Statistics.
- Crist, E.P., Cicone, R.C., 1984. A physically-based transformation of thematic mapper data—the TM tasseled cap. *IEEE Trans. Geosci. Remote Sens.* 3, 256–263.
- Definiens, A.G., 2009. Definiens eCognition developer 8 user guide. Definiens AG, München, Germany.
- Duro, D.C., Franklin, S.E., Dubé, M.G., 2012. A comparison of pixel-based and object-based image analysis with selected machine learning algorithms for the classification of agricultural landscapes using SPOT-5 HRG imagery. *Remote Sens. Environ.* 118, 259–272.
- Ecological Stratification Working Group (Canada), Center for Land, Biological Resources Research (Canada), & Canada. State of the Environment Directorate, 1996. A National Ecological Framework for Canada. Centre for Land and Biological Resources Research. State of the Environment Directorate, Hull, Quebec.
- Erwin, K.L., 2009. Wetlands and global climate change: the role of wetland restoration in a changing world. *Wetlands Ecol. Manage.* 17 (1), 71.
- Fay, M.P., Proschak, M.A., 2010. Wilcoxon-Mann-Whitney or t-test? On assumptions for hypothesis tests and multiple interpretations of decision rules. *Stat. Surv.* 4, 1.
- Filella, I., Penuelas, J., 1994. The red edge position and shape as indicators of plant chlorophyll content, biomass and hydric status. *Int. J. Remote Sens.* 15 (7), 1459–1470.
- Finlayson, C.M., Davidson, N.C., Spiers, A.G., Stevenson, N.J., 1999. Global wetland inventory—current status and future priorities. *Mar. Freshw. Res.* 50 (8), 717–727.
- Gallant, A.L., 2015. The challenges of remote monitoring of wetlands. *Remote Sens.* 7, 10938–10950.
- Gascon, F., Bouzinac, C., Thépaut, O., Jung, M., Francesconi, B., Louis, J., et al., 2017. Copernicus Sentinel-2A calibration and products validation status. *Remote Sensing* 9 (6), 584.
- Guo, M., Li, J., Sheng, C., Xu, J., Wu, L., 2017. A review of wetland remote sensing. *Sensors* 17 (4), 777.
- Harken, J., Sugumaran, R., 2005. Classification of Iowa wetlands using an airborne hyperspectral image: a comparison of the spectral angle mapper classifier and an object-oriented approach. *Can. J. Remote Sens.* 31 (2), 167–174.
- Hay, G.J., Castilla, G., 2008. Geographic Object-Based Image Analysis (GEOBIA): a new name for a new discipline. *Object-Based Image Anal.* 75–89.
- Iwasaki, A., Tonooka, H., 2005. Validation of a crosstalk correction algorithm for ASTER/SWIR. *IEEE Trans. Geosci. Remote Sens.* 43 (12), 2747–2751.
- Laba, M., Blair, B., Downs, R., Monger, B., Philpot, W., Smith, S., et al., 2010. Use of textural measurements to map invasive wetland plants in the Hudson River National

- Estuarine Research Reserve with IKONOS satellite imagery. *Remote Sens. Environ.* 114 (4), 876–886.
- Leblanc, M., Lemoal, J., Bader, J.C., Tweed, S., Mofor, L., 2011. Thermal remote sensing of water under flooded vegetation: New observations of inundation patterns for the 'Small' Lake Chad. *J. Hydrol.* 404 (1), 87–98.
- Lehmann, E.L., 2004. Elements of Large-Sample Theory. Springer Science & Business Media.
- Li, Y., Chen, J., Ma, Q., Zhang, H.K., Liu, J., 2018. Evaluation of Sentinel-2A surface reflectance derived using Sen2Cor in North America. *IEEE J. Sel. Top. Appl. Earth Obs. Remote Sens.* 99, 1–25.
- Mahdavi, S., Salehi, B., Amani, M., Granger, J.E., Brisco, B., Huang, W., Hanson, A., 2017a. Object-based classification of Wetlands in Newfoundland and labrador using multi-temporal PolSAR data. *Can. J. Remote Sens.* 1–19.
- Mahdavi, S., Salehi, B., Granger, J., Amani, M., Brisco, B., 2017b. Remote sensing for wetland classification: a comprehensive review. *GISci. Remote Sens.* 1–36.
- Mahdianpari, M., Salehi, B., Mohammadimane, F., Motagh, M., 2017. Random forest wetland classification using ALOS-2 L-band, RADARSAT-2 C-band, and TerraSAR-X imagery. *ISPRS J. Photogramm. Remote Sens.* 130, 13–31.
- Mahdianpari, M., Salehi, B., Mohammadimane, F., Brisco, B., Mahdavi, S., Amani, M., Granger, J.E., 2018. Fisher linear discriminant analysis of coherency matrix for wetland classification using PolSAR imagery. *Remote Sens. Environ.* 206, 300–317.
- Manevski, K., Manakos, I., Petropoulos, G.P., Kalaitzidis, C., 2011. Discrimination of common Mediterranean plant species using field spectroradiometry. *Int. J. Appl. Earth Observ. Geoinf.* 13 (6), 922–933.
- Marton, J.M., Creed, I.F., Lewis, D.B., Lane, C.R., Basu, N.B., Cohen, M.J., Craft, C.B., 2015. Geographically isolated wetlands are important biogeochemical reactors on the landscape. *Bioscience* 65 (4), 408–418.
- Minitab, C., 1991. Minitab Reference Manual (Release 7.1). State Coll., PA16801, USA.
- Mitsch, W.J., Gosselink, J.G., 2000. Wetlands, third ed. Wiley, New York.
- Mutanga, O., Skidmore, A.K., 2007. Red edge shift and biochemical content in grass canopies. *ISPRS J. Photogramm. Remote Sens.* 62 (1), 34–42.
- Mutanga, O., Adam, E., Cho, M.A., 2012. High density biomass estimation for wetland vegetation using WorldView-2 imagery and random forest regression algorithm. *Int. J. Appl. Earth Observ. Geoinf.* 18, 399–406.
- Mwangi, B., Tian, T.S., Soares, J.C., 2014. A review of feature reduction techniques in neuroimaging. *Neuroinformatics* 12 (2), 229–244.
- National Wetlands Working Group. Canada Committee on Ecological (Biophysical) Land Classification, 1987. The Canadian Wetland Classification System. Lands Conservation Branch, Canadian Wildlife Service, Environment Canada.
- Ozesmi, S.L., Bauer, M.E., 2002. Satellite remote sensing of wetlands. *Wetlands Ecol. Manage.* 10 (5), 381–402.
- Proctor, C., He, Y., Robinson, V., 2013. Texture augmented detection of macrophyte species using decision trees. *ISPRS J. Photogramm. Remote Sens.* 80, 10–20.
- Richter, R., 2011. Atmospheric/Topographic fro Satellite Imagery (ATCOR 2/3 User Guide, Version 8). DLR-German Aerospace Center, Wessling, Germany.
- Ryan, B.F., Joiner, B.L., 2001. Minitab Handbook. Duxbury Press.
- Schmidt, K.S., Skidmore, A.K., 2003. Spectral discrimination of vegetation types in a coastal wetland. *Remote Sens. Environ.* 85 (1), 92–108.
- Shettigara, V.K., Kempinger, S.G., Aitchison, R., 1995. Semi-Automatic detection and extraction of man-made objects in multispectral aerial and satellite images. In: Automatic Extraction of Man-Made Objects from Aerial and Space Imagespp. 63–72.
- Smith, K.B., Smith, C.E., Forest, S.F., Richard, A.J., 2007. A Field Guide to the Wetlands of the Boreal Plains Ecozone of Canada. Ducks Unlimited Canada, Western Boreal Office, Edmonton, Alberta.
- South, R., 1983. Biogeography and Ecology of the Island of Newfoundland. 48. Springer Science & Business Media.
- Tiner, R.W., Lang, M.W., Klemas, V.V. (Eds.), 2015. Remote Sensing of Wetlands: Applications and Advances. CRC Press.
- Yeung, K.Y., Bumgarner, R.E., Raftery, A.E., 2005. Bayesian model averaging: development of an improved multi-class, gene selection and classification tool for microarray data. *Bioinformatics* 21 (10), 2394–2402.